Evaluation of New CBCT Image Reconstruction Algorithms for Proton Adaptive Therapy Workflows

2026 JULY 19–22 VANCOUVER, BC
JOINT AAPM | COMP MEETING

J. Pakela, P. Klages, A. Ayan and E. Lee
The Ohio State University, Department of Radiation Oncology, Columbus, OH

The James
The Ohio State University
Comprehensive Cancer Center

INTRODUCTION

New ProBeam 360º CBCT reconstruction algorithms—iCBCT, iCBCT Acuros, and iCBCT MAR Adaptive—have been developed. The imaging performance, Hounsfield Unit (HU) accuracy, and proton-dose calculation implications were evaluated in comparison with the standard filtered back-projection algorithm. The goal is to ultimately characterize image quality, assess metal-artifact mitigation, and determine suitability for CBCT-based synthetic CT generation and proton adaptive radiotherapy workflows.

METHOD

A Gammex electron-density phantom and three anthropomorphic phantoms (head, thorax, pelvis) were scanned on the ProBeam 360º CBCT system using four reconstruction algorithms. Each imaging protocol was repeated across anatomical sites using identical acquisition parameters (125 kV, site-specific mAs). Corresponding reference CT scans were acquired on a Siemens go.Open Pro CT scanner. HU values for all Gammex tissue substitutes and selected anatomical regions were compared between CBCTs and CT. Proton treatment plans were created on the reference CTs for head and thorax phantoms and recalculated on each CBCT dataset to evaluate dose deviations and sensitivity to reconstruction algorithm choice.

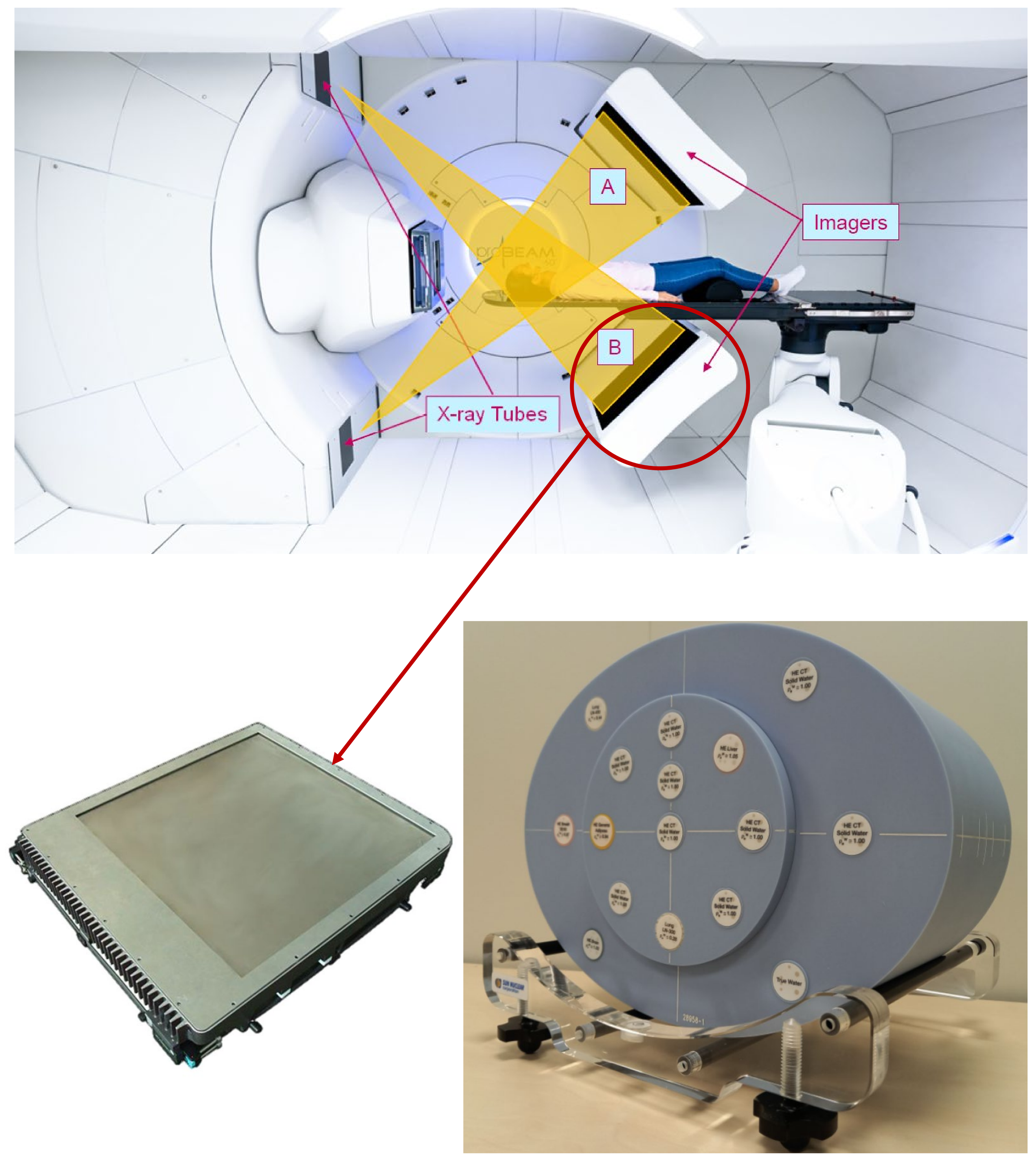

Figure 1 A gantry treatment room imaging system at the Ohio State University proton therapy center and Gammex Advanced Electron Density phantom

RESULTS

The overall shape of the calibration curves remained consistent with the commissioning CT calibration across the entire density range (Figure 2). For densities below approximately 1.1 g/cm³, corresponding to lung and soft tissues, all reconstruction algorithms closely tracked the commissioning CT curve. Greater divergence emerged for high-density inserts, particularly $CaCO_3$ and cortical bone materials. The largest deviations occurred for MAR Adaptive and Acuros in cortical bone and for Standard and iCBCT in the $CaCO_3$ 50% insert. For lung-equivalent and soft-tissue-equivalent inserts, MAR Adaptive and Acuros generally demonstrated deviations within approximately ±12 HU. Dense materials exhibited substantially larger reconstruction-dependent errors. The largest positive deviation of 116 HU was observed for iCBCT in the $CaCO_3$ 50% insert, whereas the largest negative deviation of -115 HU occurred for MAR Adaptive in cortical bone (Figure 3). To investigate whether the commissioning CT calibration may be directly applied to each CBCT reconstruction, HU values were converted back to mass density using the planning CT calibration and compared with the known phantom densities (Figure 4). Most soft-tissue inserts demonstrated density deviations less than approximately ±2%. Larger deviations appeared in high-density inserts, reaching approximately 3.5% in cortical bone and calcium-containing inserts. Quantitatively assessing the treatment plans generated using anthropomorphic phantoms found the max dose differences (cGy RBE) between the reference and CBCT-forward calculated plan occurred for the standard algorithm, with the lowest dose-differences exhibited by the iCBCT MAR Adaptive and iCBCT Acruos algorithms for the head and thorax plans, respectively.

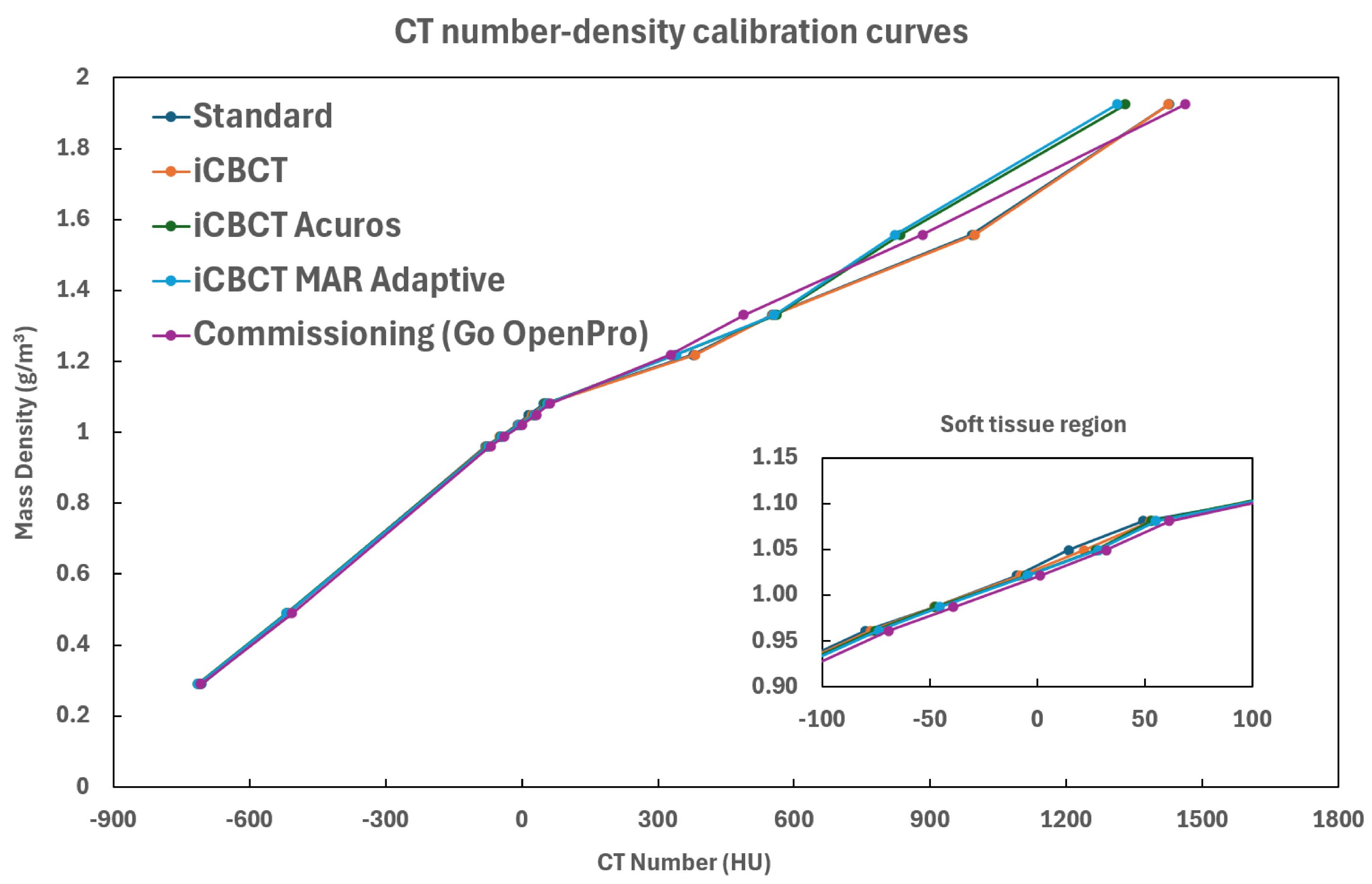

Figure 2 CT number–density calibration curves for commissioning CT, iCBCT, iCBCT Acuros, iCBCT MAR Adaptive, and Standard CBCT reconstruction.

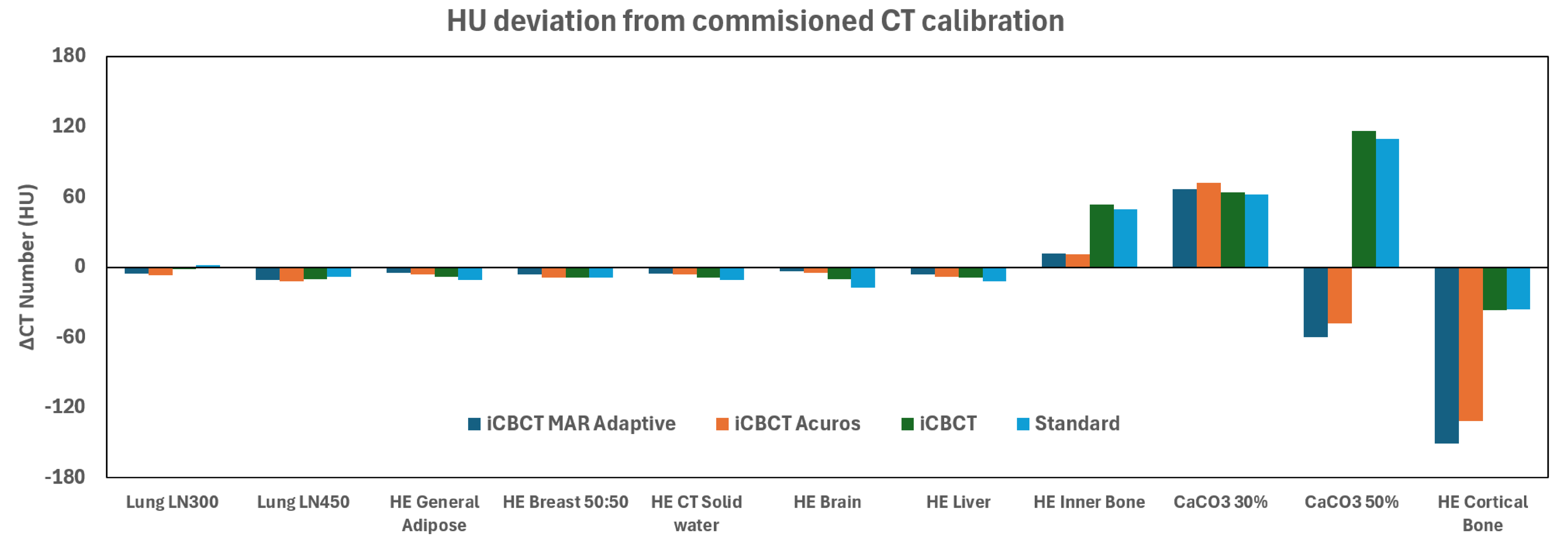

Figure 3 HU deviation relative to commissioning CT as a function of mass density.

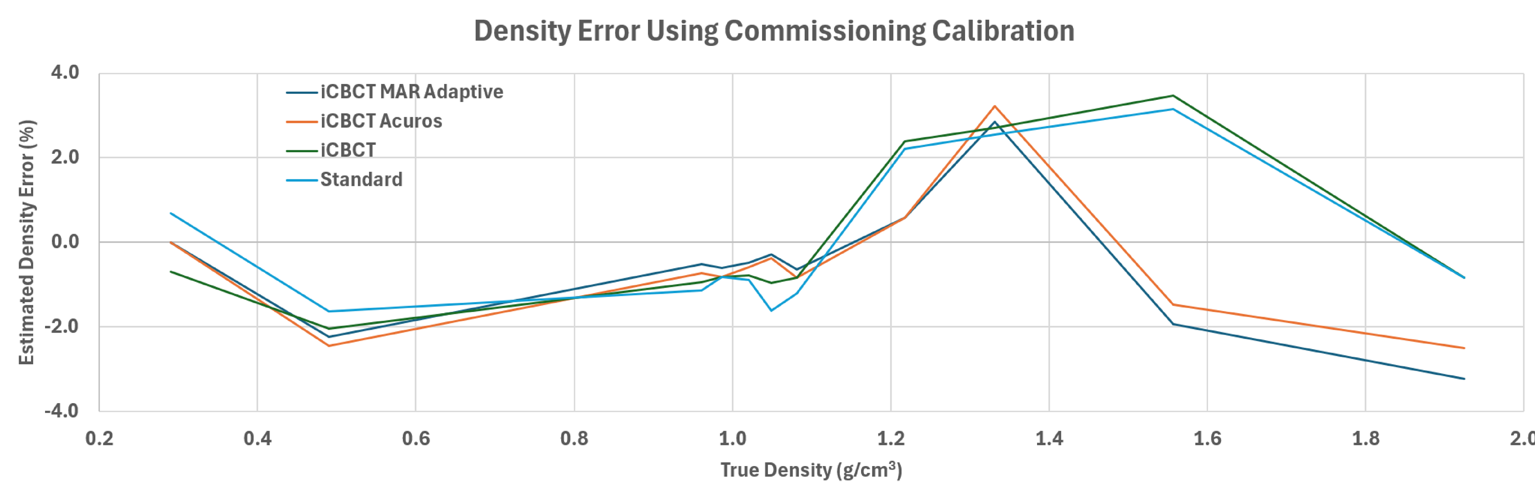

Figure 4 Estimated density error obtained when CBCT HU values are converted using the commissioning CT calibration curve.

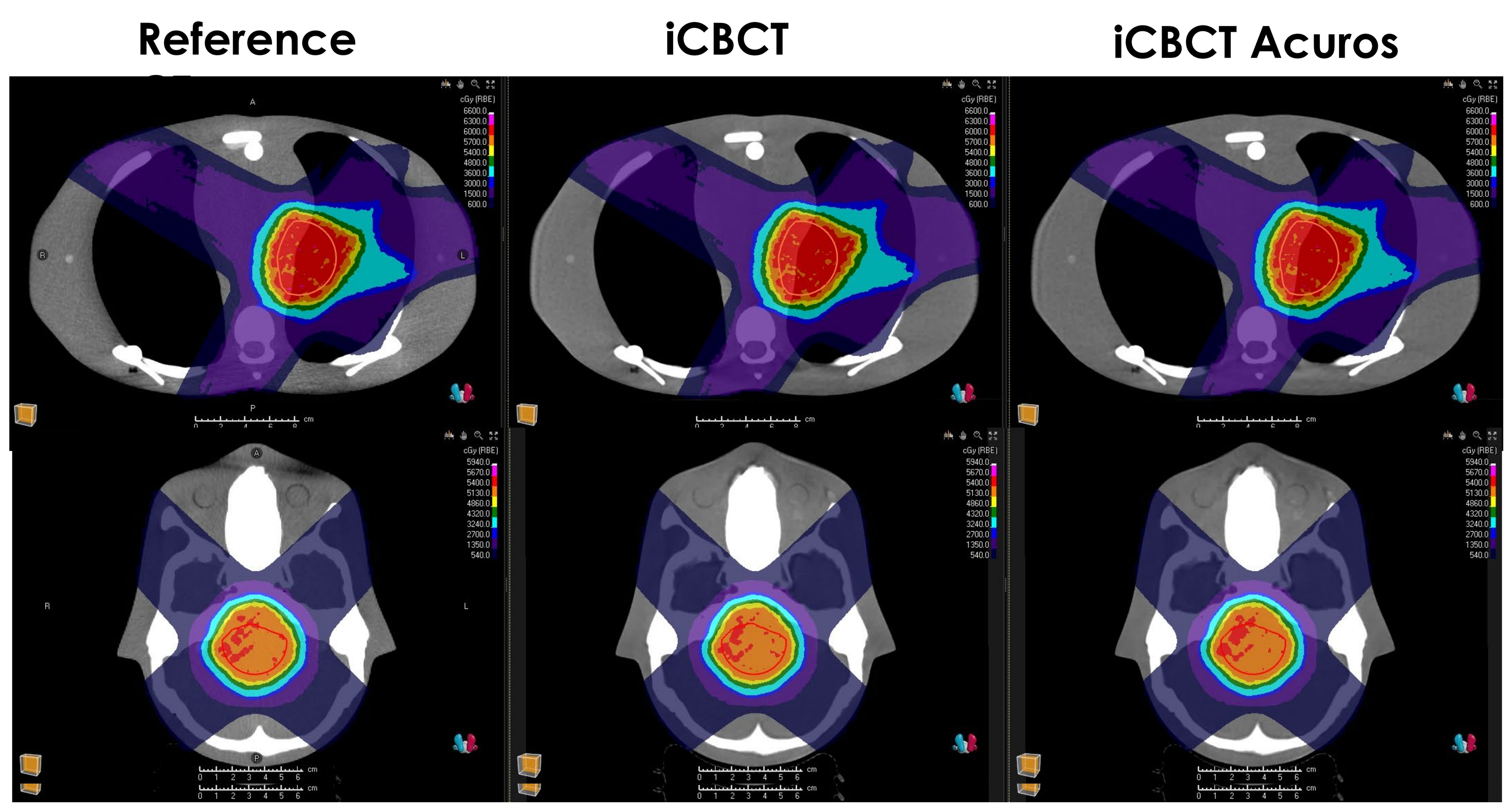

Figure 5 Computed dose comparison on thorax (top) and head (bottom) anthropomorphic phantom.

Table 1 Maximum % dose differences between the plan CT and the CBCT reconstruction methods for a brain plan and a thorax plan.

	Head	Thorax
Standard	8.1	-9.2
iCBCT	7.1	-7.2
iCBCT Acuros	5.9	5.7
iCBCT MAR Adaptive	5.7	-6.5

CONCLUSIONS

The iCBCT-based reconstruction algorithms class exhibits potential fidelity with the reference CT images. Further work is necessary to understand the conditions under which these algorithms are acceptable for proton dose calculation in an adaptive paradigm.

CONTACT INFORMATION

Eunsin Lee, PhD, DABR
The Ohio State University Department of Radiation Oncology
Office: (614) 814-9645 | Email: Eunsin.Lee@osumc.edu